



ELSEVIER

Available online at www.sciencedirect.com

SCIENCE @ DIRECT®

Journal of Magnetism and Magnetic Materials 286 (2005) 65–71

Journal of
magnetism
and
magnetic
materials

www.elsevier.com/locate/jmmm

Tunable thermal hysteresis in magnetic multilayers: magnetic superheating and supercooling

R.E. Camley^{a,*}, W. Lohstroh^b, G.P. Felcher^c, N. Hosoi^d, H. Hashizume^d

^aDepartment of Physics, University of Colorado at Colorado Springs, 1420 Austin Bluffs Parkway, P.O. Box 7150, Colorado Springs, CO 80933-7150, USA

^bVrije Universiteit, De Boelelaan 1081, 1081 HV Amsterdam, The Netherlands

^cMaterial Science Division, Argonne National Laboratory, Argonne, IL 60439, USA

^dResearch and Education Center for Materials Science, Nara Institute of Science and Technology, Ikoma 630-0192, Japan

Available online 22 October 2004

Abstract

The phenomena of superheating and supercooling can lead to a thermal hysteresis curve where two states are stable over a range of temperatures. Here we present a simple magnetic multilayer system (Fe/Gd) that can be *designed* to show a thermal hysteresis curve. Calculations show that, with proper choice of parameters, the width, in temperature, of the hysteresis curve can be controlled by an external magnetic field and varies from 20 to 100 K over a field range of 300–600 Oe. Polarized neutron reflectivity measurements confirm that such behavior is realized experimentally in multilayers of Fe/Gd.

© 2004 Elsevier B.V. All rights reserved.

PACS: 75.25.+z; 75.70.-I; 75.75.+a

Keywords: Fe; Gd; Magnetic multilayers; Thermal hysteresis

Superheating and supercooling are well-known phenomena. Most of the examples of superheating and supercooling concern physical changes of state such as melting or crystallization [1]. A magnetic example of supercooling has been discussed recently regarding magnetic phase transitions in

erbium [2]. In magnetism one can also find discussions of high- and low-spin transitions in molecules that have an associated thermal hysteresis [3]. Many of these systems have a requirement of ultrapure samples since impurities can act as nucleation sites and initiate the phase transition.

Here we present a simple magnetic multilayer system that can be *designed* to show a thermal hysteresis curve. The width, in temperature, of this hysteresis curve can be controlled by an external

*Corresponding author. Tel.: +1 719 262 3512; fax: +1 719 262 3013.

E-mail address: rcamley@uccs.edu (R.E. Camley).

magnetic field with small fields (200–300 Oe) leading to thermal hysteresis spanning about a hundred degrees Kelvin. Larger fields (600 Oe and above) reduce the width of the hysteresis curve to 20 K.

We consider a multilayer system with alternating ferromagnetic films that are antiferromagnetically coupled at the interfaces. In addition it is necessary that the magnetization of one material change more rapidly with temperature than the other. An example of such a system is the Fe/Gd multilayer where Gd thermal averaged magnetic moment changes from $7\mu_B$ to zero as T changes from 0 to about 300 K. There are a number of known magnetic states for the Fe/Gd system [4–6] which are illustrated in Fig. 1. There is a low-temperature aligned-Gd state where the Gd magnetization is aligned with the external field (and the Fe is opposite) and there is a high temperature aligned-Fe state where the Fe magnetization is aligned with the external field. These configurations are stable when the applied magnetic field is small; in higher magnetic fields there is a spin-flop like state where the Fe and Gd moments are both canted with respect to the applied field.

The physical origin for the thermal hysteresis is simple. At high temperatures the system is in the Fe-aligned state; the Gd moments, which are small, are oppositely directed to the field. As the temperature decreases the Gd moments increase and the net magnetic moment can actually be opposite to the external field if an anisotropy in Fe

holds the Fe spins in place. Eventually, however, this configuration becomes unstable and the structure reverses with the Gd moments along the field and the Fe moments antiparallel to the applied field. A similar situation occurs on heating the system from low temperatures.

The general situation of a Fe/Gd multilayer is quite complicated and, in fact, shows dramatic surface effects, as we shall see. We can, however, obtain some useful intuition using a simple model which includes the Zeeman energy of each film in the applied field, the interfacial exchange energy between the two films and a uniaxial anisotropy in film 1 (Fe).

$$E = -H * (t_1 m_1 \cos \theta_1 + t_2 m_2 \cos \theta_2) - J m_1 m_2 \cos(\theta_2 - \theta_1) - t_1 m_1 H_a \cos^2 \theta_1. \quad (1)$$

Here H is the external magnetic field, t_1 the thickness of film 1, m_1 the magnetization of film 1 and θ_1 is the angle between m_1 and the external field. Similar definitions hold for the 2nd material. H_a is the anisotropy field, assumed to exist in film 1 (Fe) only for simplicity, and assumed to be in the same direction of the measuring field. We note that Gd is in an S state and therefore the anisotropy is expected to be small. In practice anisotropy can be induced by different types of growth methods (deposition in a magnetic field, tilting the substrate during deposition, etc.). However, the general features obtained here should persist if the anisotropy is found in the Fe, in both materials, or only in the Gd. J measures the exchange coupling between films and is negative for antiferromagnetic coupling.

To have a stable magnetic state we require the usual conditions that $E(\theta_1, \theta_2)$ is a minimum

$$\frac{\partial E}{\partial \theta_1} = \frac{\partial E}{\partial \theta_2} = 0, \quad (2)$$

and

$$\frac{\partial^2 E}{\partial \theta_1^2} > 0 \text{ and } \frac{\partial^2 E}{\partial \theta_2^2} > 0, \quad (3)$$

and

$$\left(\frac{\partial^2 E}{\partial \theta_1^2} \right) \left(\frac{\partial^2 E}{\partial \theta_2^2} \right) > \left(\frac{\partial^2 E}{\partial \theta_1 \partial \theta_2} \right)^2. \quad (4)$$

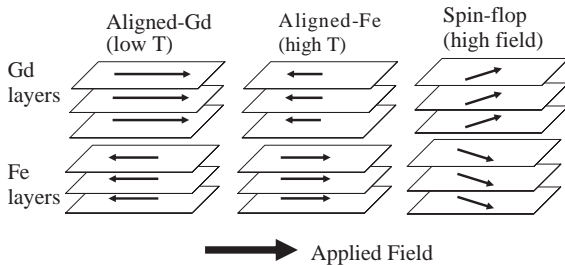


Fig. 1. Illustration of the three main phases in the Fe/Gd superlattice. In the Gd-aligned phase the thermal averaged moments of the Gd are large and aligned with the external field. In the Fe-aligned phase at higher temperature the Gd moments are small and the Fe moments align with the field.

It is easy to show that Eqs. (2) and (3) are satisfied by either the Fe-aligned state ($\theta_1=0, \theta_2=\pi$), or by the Gd-aligned state ($\theta_1=\pi, \theta_2=0$), as long as the external field is small compared to the exchange field. The critical condition of Eq. (4) can be found using Eq. (1) and solved for m_2 , the moment in the Gd film. After some algebra, we find

$$m_2 = \frac{t_1(\pm H^2 t_2 + m_1 H J + 2H_a H t_2 \pm 2H_a m_1 J)}{J t_2 H} \quad (5)$$

Here the + sign indicates the critical value of m_2 for the high-temperature state (Fe-aligned) and the – sign indicates the critical value for the low-temperature state (Gd-aligned).

We show the stability limits from Eq. (5) in Fig. 2. The parameters for the calculation are chosen to reasonably match the experimental conditions discussed below. The thickness of the Fe film is $t_1 = 35 \times 10^{-8}$ cm; the thickness of the Gd film is $t_2 = 50 \times 10^{-8}$ cm; the uniaxial anisotropy in Fe is $H_a = 50$ G. The magnetization in Fe is assumed to

be constant over the temperature range measured and is given by $m_1 = 1740$ G. Thus this figure shows the values of the Gd magnetization at which the different states become unstable. For example, at low applied field the Gd-aligned state is stable for m_2 values above the lower curve, and the Fe-aligned state is stable for m_2 values below the upper curve. There is also a range of Gd magnetization values where both states are stable. This range of magnetization values corresponds to a range of temperatures since the Gd magnetization changes rapidly with temperature. Because there are two stable states in this temperature range, one has the possibility of thermal hysteresis. As the applied field is increased, this region where the two states are simultaneously stable becomes much smaller. This shows that the thermal hysteresis curve ought to narrow substantially at higher fields. In fact, by setting the two critical values in Eq. (5) equal to each other, we can obtain an equation for the maximum applied field which allows thermal hysteresis. We find

$$H_m = \sqrt{-2H_a m_1 J / t_2} \quad (6)$$

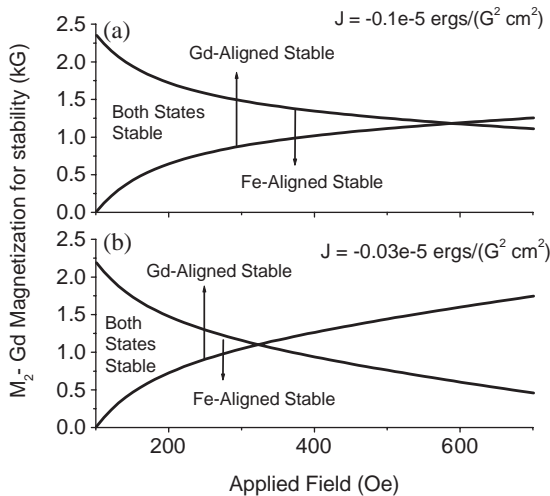


Fig. 2. Stability limits for the Fe- and Gd-aligned states as a function of applied magnetic field. At low applied fields both states are stable over a range of magnetization values for Gd. (a) shows the phase diagram for a larger antiferromagnetic interfacial coupling and (b) shows the phase diagram for smaller antiferromagnetic interfacial coupling. As the antiferromagnetic coupling is increased the region where both states are stable also increases.

A comparison of Fig. 2(a) and (b) shows the effect of interfacial exchange on the stability regions for the different states. The most noticeable feature is that when the exchange coupling is weaker, the region where both aligned states are stable is restricted to a smaller range of applied field values. The reason for this is that a weaker interfacial exchange allows the canting of spins at the interface at lower applied fields. The aligned states become unstable and the spin flop state is the only one allowed. Similarly, a reduction of the anisotropy also reduces the range for thermal hysteresis in agreement with Eq. (6).

We can make a direct connection between the results in Fig. 2 and the temperature range over which both states are stable by using a graph for magnetization as a function of temperature for Gd as shown in Fig. 3. For example, at $H = 200$ Oe in part (b) of Fig. 2 we see that both states are stable when the Gd magnetization is between 0.73 and 1.47 kG. Using Fig. 3, we can see these magnetization values correspond to temperatures of 272 and 200 K, a range of 72 K.

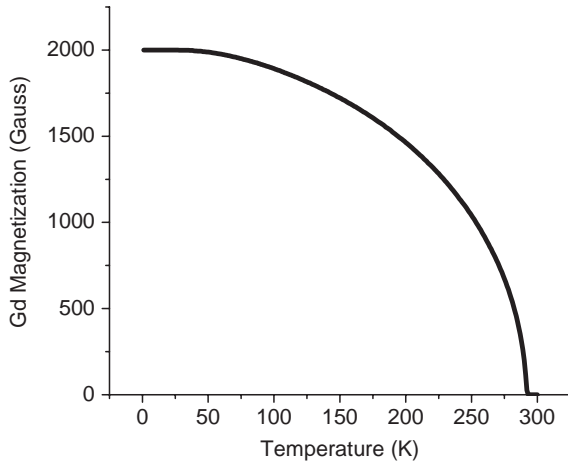


Fig. 3. Theoretical calculation for $M(T)$ for Gd.

The calculation associated with Eqs. (1)–(5) assumes that the spins within a film are rigidly locked together. If the exchange coupling between films is significant, this may not be a good assumption. We therefore examine the thermal hysteresis in the Fe/Gd system using a self-consistent local mean-field method that has been used successfully by a number of groups to describe this system [4–7].

In this model we consider alternate films of BCC Fe and HCP Gd. The spins in each monolayer are ferromagnetically ordered and lie parallel to the film surfaces. Only nearest-neighbor exchange interactions are considered. A spin in monolayer i feels a total field composed of the exchange fields from the layers above and below, external fields and anisotropy fields:

$$\vec{H}_i = \sum_{nm} (J_{i,i+1} \langle \vec{S}_{i+1} \rangle + J_{i,i-1} \langle \vec{S}_{i-1} \rangle) + H\hat{z} + H_a \langle S_i^z \rangle / S_i. \quad (7)$$

We use an anisotropy of 50 G in Fe and H_a is taken to be zero in Gd. All other parameters are given in Ref. [4]. (The reduction parameter of Ref. [4] is 0.75.). The minimum energy state is found using an iterative method where a layer of spins is chosen at random. One finds the net effective field acting on this layer and the spins in the layer are rotated to lie along this field. This lowers the energy of the system. The process is repeated until a self-consistent state is reached where the spins in

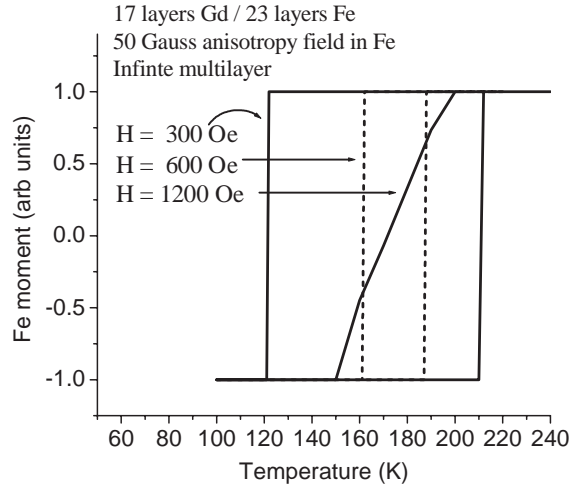


Fig. 4. Theoretical thermal hysteresis curves for a 17 ML Gd / 23 ML Fe superlattice for different applied magnetic fields. The hysteresis curves initially narrow as the applied field is increased. At higher fields (1200 Oe) the system is in a spin-flop phase and does not show substantial hysteresis.

each layer are aligned with the effective fields produced by the external field, the anisotropy fields and the exchange fields of the neighboring layers. To take temperature into account, the thermal averaged magnitude $\langle S_i \rangle$ is given by the Brillouin function $\langle S_i \rangle = S_i B(S_i H_i / kT)$.

The results for the Fe magnetization as a function of temperature for an infinite Fe/Gd superlattice are given in Fig. 4. This curve is calculated for a structure with 17 monolayers Gd and 23 monolayers of Fe in each unit cell. Again this choice of values is intended to match the experimental parameters of Gd 50 Å / Fe 35 Å. (We assume c -axis growth for the Gd with a lattice parameter of 5.78 Å and two layers per unit cell; for Fe the layer to layer distance is about 1.43 Å). The uniaxial anisotropy in Fe is taken as 50 G. Periodic boundary conditions are used to simulate the infinite superlattice. The width of the hysteresis curve is quite large for low magnetic fields and becomes narrower at higher fields in agreement with the results of Fig. 2. For even higher fields the system does not display hysteresis, but makes a transition from the aligned phases to the spin flop phase and the magnetization essentially increases linearly as a function of temperature. Again this is

in agreement with Fig. 2 where we have seen that neither the Gd-aligned nor the Fe-aligned state is stable in the high-field region of the phase diagram.

It is known that the finite size of a Fe/Gd superlattice can have a significant influence on the phase transitions. For example, at low temperatures and low fields the system is typically in the Gd-aligned state. If the magnetic field is increased the magnetic structure will eventually change to a spin-flop-like state. However, the critical field at which this phase transition takes place depends dramatically on whether the outermost surface is Gd terminated or Fe terminated. If the structure has Fe spins on the outside, then in the Gd-aligned state the Fe spins are opposite to the external field and a surface phase transition to the spin flop state nucleates at the Fe surface [8–10]. The critical field for this surface transition is about a factor of 5 lower than that for the bulk transition.

The thermal hysteresis effect discussed here also shows substantial finite size effects. In Fig. 5, we compare results for an infinitely extended multilayer with a unit cell 17 ML Gd/23 ML Fe with those of a finite multilayer with the same unit cell but with a total of 15 repetitions. The thermal hysteresis for an infinite structure is approximately

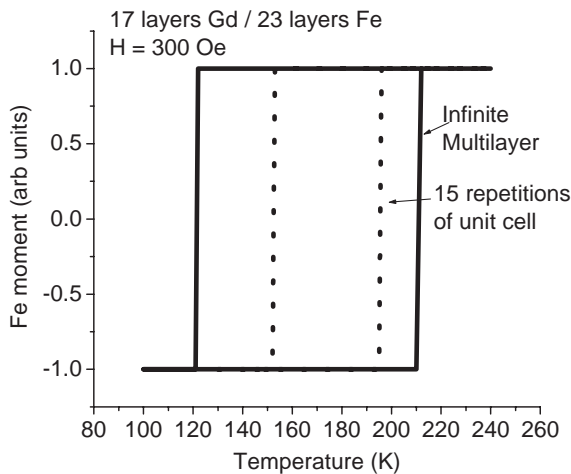


Fig. 5. Theoretical thermal hysteresis curves for a finite and infinite Fe/Gd multilayer. The unit cell is 17 ML Gd/23 ML Fe in both cases. The applied field is 300 Oe. We note that the finite multilayer has a substantially narrower thermal hysteresis curve.

twice as wide as that for the finite structure. This is due to the surface phase transition discussed above. In a finite structure composed simply of a repetition of the Fe/Gd unit cell, the spins at one surface will always be opposite to the applied field in an aligned state, and as a result a surface phase transition will nucleate at that surface. These surface effects will be discussed in detail elsewhere. Nonetheless, the main features of the thermal hysteresis remain qualitatively the same regardless of the number of unit cells, and it is important to compare our theoretical results with the results of an experiment. In fact, in a related system, a thermal hysteresis curve has already been seen in a reorientation transition [11] of ultrathin Fe on Gd.

Measurements were taken on a multilayer with composition [Gd 50 Å/Fe 35 Å] × 15 deposited on a Si wafer with Fe as the top layer of the multilayered stack. The sample was covered with 40 Å Si to prevent oxidation. X-ray reflectometry confirms a well ordered sample with flat interfaces (rms-roughness 7 Å). The compensation temperature was determined to be 125 K by Squid magnetometry. The magnetic properties were studied with polarized neutron reflectometry at the Intense Pulsed Neutron Source of Argonne National Laboratory. Fig. 6 presents the intensity of the first Bragg reflection of the superlattice as a function of the neutron momentum transfer

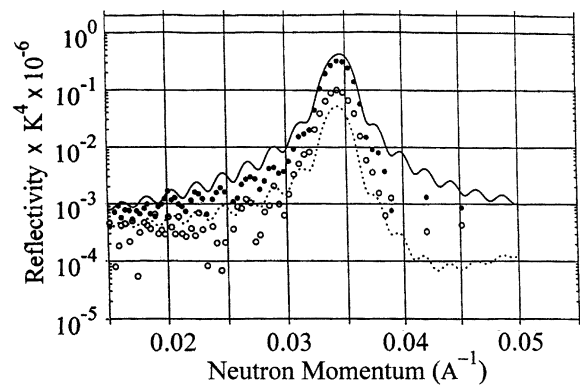


Fig. 6. The spin-dependent neutron reflectivities in the region of the first Bragg reflection for the two polarization states of the neutron. R^+ (black circles) is the reflectivity for the case where the incident neutrons are polarized parallel to the applied field and R^- (open circles) refers to incident electrons polarized antiparallel to the applied field.

perpendicular to the surface, for the two polarization states of the neutron [12]. The width of the peak, which is inversely proportional to the number of layers coherently diffracting neutrons, as well as the presence of secondary oscillations, due to the total superlattice thickness, indicate the high perfection of the sample.

In the Fe aligned state the intensities diffracted at the first Bragg peak are proportional to a combination of the scattering amplitudes of the single bilayer:

$$I^{\pm} \propto [(N_{\text{Fe}}b_{\text{Fe}} - N_{\text{Gd}}b_{\text{Gd}}) \pm (|N_{\text{Fe}}p_{\text{Fe}}| + |N_{\text{Gd}}p_{\text{Gd}}|)]^2, \quad (8)$$

whereas for Gd aligned in field direction the intensities are proportional to:

$$I^{\pm} \propto [(N_{\text{Fe}}b_{\text{Fe}} - N_{\text{Gd}}b_{\text{Gd}}) \mp (|N_{\text{Fe}}p_{\text{Fe}}| + |N_{\text{Gd}}p_{\text{Gd}}|)]^2, \quad (9)$$

$b_{\text{Fe,Gd}}$ are the nuclear and $p_{\text{Fe,Gd}}$ the magnetic scattering lengths for the two elements that are assumed aligned in the direction of the applied field. A convenient quantity is the spin asymmetry $P = (I^+ - I^-)/(I^+ + I^-)$, which is basically proportional to the magnetization of the Fe sublattice, and thus it can be immediately compared with the theoretical predictions. Fig. 7 shows the spin asymmetry when the sample is cycled as a function of temperature at different fields. For $H < 1200$ Oe the loop shows hysteresis. The area subtended by the loop decreases as the field is increased; yet the slope

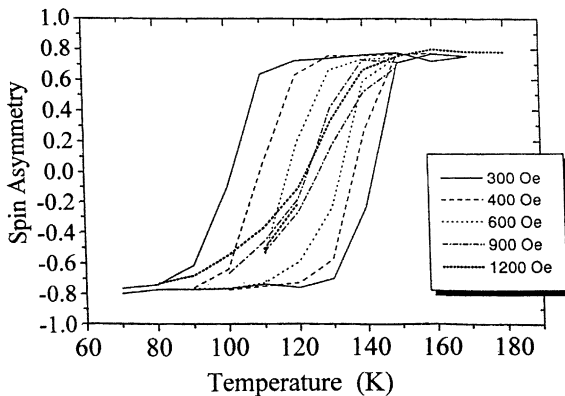


Fig. 7. Thermal hysteresis of the asymmetry P . The vertical axis is proportional to the Fe magnetization.

of the segments uniting the lower to the upper branch remains the same. Above 900 Oe the loop has closed down almost completely, but with a smoother transition from the lower to the upper branch.

The results presented here show the excellent qualitative agreement of theory and experiments, particularly in that the width of the thermal hysteresis decreases as the external field is increased, and in the transition to the spin flop state at higher fields, a state where the magnetization increases approximately linearly with temperature.

It would be desirable to have a direct experimental confirmation that at low field the magnetization simply reverses, while at higher fields the magnetization reverses by gradual rotation, from an aligned state to a spin-flop configuration to a reversed aligned state. This verification was not possible in our experiments due to technical reasons. During reversal, the system breaks down in domains of ~ 1000 Å lateral dimension. These cause broadening of the reflected beam. The total intensity is recorded accurately by the detector, but the used supermirror polarization analyzer operates correctly only on well-collimated beams. An experimental check with a ^3He -polarization analyzer which accepts a broad angular spread of the reflected beam would be desirable to check the spin-flop transition. However, even without that verification, abundant evidence for this transition already exists [13–18].

In summary we have demonstrated both theoretically and experimentally a novel system which has a thermal hysteresis curve that can be significantly changed by application of an external magnetic field. Although the present work deals with a specific system, Fe/Gd, it is applicable to a whole set of layered structures where the temperature dependence of one material is substantially different from that of the other.

Acknowledgments

The work by REC was supported by a grant from the ARO Grant #DAAD19-02-1-0174. The work by GPF was supported by US DOE, Office of Science Contract W31-109-ENG-38. WL ac-

knowledges financial support by NATO CRG programme SA (CRG.CRG.973129).

References

- [1] Z.H. Zhang, P. Kulatunga, H.E. Elsayed-Ali, Phys. Rev. Lett. 56 (1997) 4141.
- [2] K.A. Gschneidner Jr., V.K. Pecharsky, David Fort, Phys. Rev. Lett. 78 (1997) 4281.
- [3] O. Kahn, C. Jay Martinez, Science 279 (1998) 44.
- [4] M. Sajjeddine, Ph. Bauer, K. Cherifi, C. Dufour, G. Marchal, R.E. Camley, Phys. Rev. B 49 (1994) 8815.
- [5] See the review article by R.E. Camley, R.L. Stamps, J. Phys.: Condens. Matter 5 (1993) 3727.
- [6] R.E. Camley, D.R. Tilley, Phys. Rev. B 37 (1988) 3413; R.E. Camley, Phys. Rev. B 39 (1989) 12316.
- [7] K. Takanashi, Y. Kamiguchi, H. Fujimori, M. Motokawa, J. Phys. Soc. Jpn. 61 (1992) 3721.
- [8] J.G. LePage, R.E. Camley, Phys. Rev. Lett. 65 (1990) 1152.
- [9] D. Haskel, Y. Choi, D.R. Lee, J.C. Lang, G. Srajer, J.S. Jiang, S.D. Bader, J. Appl. Phys. 93 (2004) 6507.
- [10] W. Hahn, M. Loewenhaupt, Y.Y. Huang, G.P. Felcher, S.S.P. Parkin, Phys. Rev. B 52 (1995) 16041.
- [11] C.S. Arnold, D.P. Pappas, A.P. Popov, Phys. Rev. Lett. 83 (1999) 3305.
- [12] G.P. Felcher, J. Appl. Phys. 87 (2000) 5431.
- [13] Ph. Bauer, M. Sajjeddine, C. Dufour, K. Cherifi, G. Marchal, Ph. Mangin, Europhys. Lett. 16 (1991) 307.
- [14] F. Itoh, N. Nakamura, H. Sakurai, J. Magn. Magn. Mater. 126 (1993) 361.
- [15] N. Ishimatsu, H. Hashizume, S. Hamada, N. Hosoito, C.S. Nelson, C.T. Venkataraman, G. Srajer, J.C. Lang, Phys. Rev. B 60 (1999) 9596.
- [16] H. Sano, H. Hashizume, H. Okuda, N. Hosoito, Jpn. J. Appl. Phys. 41 (2002) 103.
- [17] N. Hosoito, H. Hashizume, N. Ishimatsu, I.-T. Bae, G. Srajer, J.C. Lang, C.K. Venkataraman, C.S. Nelson, Jpn. J. Appl. Phys. 41 (2002) 131.
- [18] N. Hosoito, H. Hashizume, N. Ishimatsu, J. Phys. Condens. Matter 14 (2002) 5289.